Quantum statistics of a single-atom Scovil–Schulz-DuBois heat engine

Sheng-Wen Li,[1,2] Moochan B. Kim,[1] Girish S. Agarwal,[1] and Marlan O. Scully[1,2]

[1]*Institute of Quantum Science and Engineering, Texas A&M University, College Station, Texas 77843, USA*

[2]*Baylor University, Waco, Texas 76798, USA*

We study the statistics of the lasing output from a single-atom quantum heat engine, which was originally proposed by Scovil and Schulz-DuBois [H. E. D. Scovil and E. O. Schulz-DuBois, Phys. Rev. Lett. **2**, 262 (1959)]. In this heat engine model, a single three-level atom is coupled with an optical cavity and is in contact with a hot and a cold heat bath together. We derive a fully quantum laser equation for this heat engine model and obtain the photon number distribution both below and above the lasing threshold. With the increase of the hot bath temperature, the population is inverted and lasing light comes out. However, we notice that if the hot bath temperature keeps increasing, the atomic decay rate is also enhanced, which weakens the lasing gain. As a result, another critical point appears at a very high temperature of the hot bath, after which the output light become thermal radiation again. To avoid this double-threshold behavior, we introduce a four-level heat engine model, where the atomic decay rate does not depend on the hot bath temperature. In this case, the lasing threshold is much easier to achieve and the double-threshold behavior disappears.

I. INTRODUCTION

In 1959, Scovil and Schulz-DuBois introduced a quantum heat engine model (the SSDB heat engine) [1,2], where a single three-level atom is in contact with two heat baths together (Fig. 1) and the population inversion between the levels $|e_1\rangle$ and $|e_2\rangle$ can be created by a large enough temperature difference giving rise to laser output. During one working cycle, one hot photon $\hbar\omega_h$ is absorbed, one cold photon $\hbar\omega_c$ is emitted, and one laser photon $\hbar\Omega_l$ is produced. Thus, they obtain the efficiency of the heat engine as $\eta_{SSDB} := \Omega_l/\omega_h$. To guarantee the laser output, a population inversion condition is required $\exp(-\frac{\omega_h}{T_h}) \geqslant \exp(-\frac{\omega_c}{T_c})$, which is obtained from the consideration of counting the Boltzmann factors. That simply leads to an upper bound for the SSDB efficiency $\eta_{SSDB} \leqslant 1 - T_c/T_h$, which is just the Carnot limit. It turns out that the SSDB heat engine is deeply connected with many other quantum heat engine models, e.g., the quantum absorption refrigerator [3–6] and the electromagnetically induced transparency based heat engine [7,8], and it also can be used to describe the photosynthesis process and solar cells [9,10].

This heat engine model gives a simple and clear demonstration of quantum thermodynamics. However, we notice that some detailed properties of this lasing heat engine, e.g., the threshold behavior and the statistics of the output light, are still not well studied. In Ref. [9], a rate equation description was developed. In order to obtain the photon statistics, we need to go beyond the rate equation description. In this paper we study this SSDB heat engine based on a more realistic single-atom lasing setup [11–15], where the three-level atom is placed in an optical cavity, is coupled with the quantized field mode, and is in contact with two heat baths with temperatures $T_{h,c}$ [16–22]. We derive the lasing equation in both semiclassical and fully quantum approaches (the Scully-Lamb approach [23–25]) and analytically obtain the photon number distribution in the steady state for both above- and below-threshold cases.

Intuitively, a higher temperature T_h from the hot bath enhances the population inversion between the two levels $|e_1\rangle$ and $|e_2\rangle$ and thus should also enhance lasing. However,

our analytical result shows that a higher temperature T_h also increases the atomic decay rate. As a result, the lasing gain decreases when T_h is too high and this system shows a double-threshold behavior: When the hot bath temperature T_h is quite low ($T_h \simeq T_c$), the excitation is too weak and the system is below the lasing threshold; with increasing T_h, population inversion happens and the lasing light comes out, but when T_h keeps increasing, the lasing gain starts to decrease and even goes below the threshold again, thus another critical point appears, after which the output light becomes thermal radiation again.

To avoid this double-threshold behavior, we study a four-level model where a third ancilla bath is introduced [26]. In this model, neither of the two lasing levels is coupled with the hot bath directly and thus the atomic decay rate no longer depends on the hot bath temperature. As a result, the lasing gain and cavity photon number increase monotonically and only one critical point exists. It turns out that the laser output of this four-level heat engine is also bounded by the Carnot efficiency.

We arrange the paper as follows. In Sec. II we introduce our model setup and give a semiclassical analysis. In Sec. III we study the fully quantum theory and derive the laser master equation. The master equation has the same structure as the Scully-Lamb master equations, however, with gain, loss, and saturation parameters specific to the three-level model of Scovil and Schulz-DuBios. In Sec. IV we present results for the photon statistics and we note the unusual feature that for a given gain, the photon distribution could be different. The quantum statistical features of the four-level model are presented in Sec. V. We conclude with a summary in Sec. VI. Detailed derivations are relegated to the Appendixes.

II. THE SSDB HEAT ENGINE

The heat engine model is demonstrated in Fig. 1 [16–18,21]. A three-level system $\hat{H}_0 = E_g|g\rangle\langle g| + E_1|e_1\rangle\langle e_1| + E_2|e_2\rangle\langle e_2|$ is placed in an optical cavity which is resonant
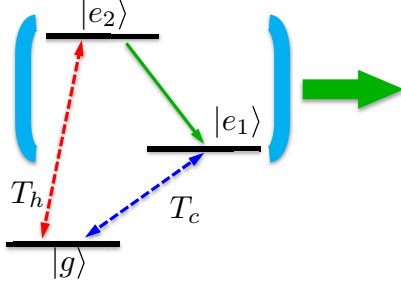
FIG. 1. Demonstration of the SSDB heat engine. A three-level atom is placed in an optical cavity to generate a laser. We define $\hbar\omega_h = E_2 - E_g$, $\hbar\omega_c = E_1 - E_g$, and $\hbar\Omega_l = E_2 - E_1$.

with the atomic transition $|e_1\rangle \leftrightarrow |e_2\rangle$. (The transition path) $|e_{1(2)}\rangle \leftrightarrow |g\rangle$ is coupled with a cold(hot) bath.

We define the atomic transition operators as $\hat{\tau}_h^- := |g\rangle\langle e_2|$, $\hat{\tau}_c^- := |g\rangle\langle e_1|$, $\hat{\sigma}^- := |e_1\rangle\langle e_2|$, $\hat{\tau}_i^+ := (\hat{\tau}_i^-)^\dagger$, and $\hat{\sigma}^+ := (\hat{\sigma}^-)^\dagger$. The atom and the cavity interact resonantly through the Jaynes-Cummings coupling $\hat{V} = g(\hat{\sigma}^+\hat{a} + \hat{\sigma}^-\hat{a}^\dagger)$ and the dynamics of this cavity-QED system can be described by the master equation (interaction picture)

$$\dot{\rho} = i[\rho,\hat{V}] + \mathcal{L}_h[\rho] + \mathcal{L}_c[\rho] + \mathcal{L}_{\mathrm{cav}}[\rho], \qquad (1)$$

where

$$\mathcal{L}_i[\rho] = \gamma_i\overline{n}_i\big(\hat{\tau}_i^+\rho\hat{\tau}_i^- - \tfrac{1}{2}\{\hat{\tau}_i^-\hat{\tau}_i^+,\rho\}\big)$$
$$\qquad + \gamma_i(\overline{n}_i + 1)\big(\hat{\tau}_i^-\rho\hat{\tau}_i^+ - \tfrac{1}{2}\{\hat{\tau}_i^+\hat{\tau}_i,\rho\}\big), \quad i = h,c$$
$$\mathcal{L}_{\mathrm{cav}}[\rho] = \kappa\big(\hat{a}\rho\hat{a}^\dagger - \tfrac{1}{2}\hat{a}^\dagger\hat{a}\rho - \tfrac{1}{2}\rho\hat{a}^\dagger\hat{a}\big). \qquad (2)$$

Here $\mathcal{L}_{h(c)}[\rho]$ is the contribution from the hot (cold) bath coupled with the atom and $\mathcal{L}_{\mathrm{cav}}[\rho]$ describes the light leaking from the cavity to the outside vacuum field. Here $\overline{n}_i := \overline{n}_P(\omega_i,T_i)$ for $i = h,c$ is the thermal photon number of the hot or cold bath calculated from the Planck distribution $\overline{n}_P(\omega,T) := [\exp(\hbar\omega/k_B T) - 1]^{-1}$. With this master equation, we obtain the equations of motion

$$\frac{d}{dt}\langle\hat{N}_1\rangle = \gamma_c[\overline{n}_c\langle\hat{N}_g\rangle - (\overline{n}_c + 1)\langle\hat{N}_1\rangle] - ig[\langle\hat{\sigma}^-\hat{a}^\dagger\rangle - \mathrm{H.c.}],$$

$$\frac{d}{dt}\langle\hat{N}_2\rangle = \gamma_h[\overline{n}_h\langle\hat{N}_g\rangle - (\overline{n}_h + 1)\langle\hat{N}_2\rangle] + ig[\langle\hat{\sigma}^-\hat{a}^\dagger\rangle - \mathrm{H.c.}],$$

$$\frac{d}{dt}\langle\hat{\sigma}^-\rangle = ig\langle\hat{\sigma}^z\hat{a}\rangle - \frac{1}{2}\Gamma\langle\hat{\sigma}^-\rangle,$$

$$\frac{d}{dt}\langle\hat{a}\rangle = -\frac{\kappa}{2}\langle\hat{a}\rangle - ig\langle\hat{\sigma}^-\rangle, \qquad (3)$$

where we define $\hat{N}_g := |g\rangle\langle g|$ and $\hat{N}_{1,2} := |e_{1,2}\rangle\langle e_{1,2}|$, $\hat{\sigma}_z := \hat{N}_2 - \hat{N}_1$ for the atom operators and

$$\Gamma := \gamma_h(\overline{n}_h + 1) + \gamma_c(\overline{n}_c + 1) \qquad (4)$$

for the atomic coherence decay rate.

We apply the semiclassical approximation that $\langle\hat{\sigma}^-\hat{a}^\dagger\rangle \simeq \langle\hat{\sigma}^-\rangle\langle\hat{a}^\dagger\rangle$ and $\langle\hat{\sigma}^z\hat{a}\rangle \simeq \langle\hat{\sigma}^z\rangle\langle\hat{a}\rangle = \langle\hat{N}_2 - \hat{N}_1\rangle\langle\hat{a}\rangle$ and assume the atom rapidly decays to its steady state right before the cavity evolves significantly. Thus the quantum coherence term is given by $\langle\hat{\sigma}^-\rangle = (2ig/\Gamma)\langle\hat{N}_2 - \hat{N}_1\rangle\langle\hat{a}\rangle$ (defining $\mathcal{E} := \langle\hat{a}\rangle$),

which is proportional to the population inversion ΔN,

$$\Delta N := \langle\hat{N}_2 - \hat{N}_1\rangle = \frac{\overline{n}_h - \overline{n}_c}{\Phi + \frac{4g^2|\mathcal{E}|^2}{\Gamma}\Psi}, \qquad (5)$$

where

$$\Psi := \frac{1}{\gamma_h\gamma_c}[\gamma_h(3\overline{n}_h + 1) + \gamma_c(3\overline{n}_c + 1)],$$
$$\Phi := 3\overline{n}_h\overline{n}_c + 2(\overline{n}_h + \overline{n}_c) + 1.$$

Notice that when there is no cavity coupling ($g = 0$), the atomic populations return to the SSDB result

$$\langle\hat{N}_g\rangle : \langle\hat{N}_1\rangle : \langle\hat{N}_2\rangle = 1 : \frac{\overline{n}_c}{\overline{n}_c + 1} : \frac{\overline{n}_h}{\overline{n}_h + 1} \qquad (6)$$

and the population inversion is

$$\Delta N_0 = (\overline{n}_h - \overline{n}_c)/\Phi. \qquad (7)$$

We see that the constant Φ is just the normalization factor.

Now we obtain the lasing equation as

$$\dot{\mathcal{E}} = \left[\frac{2g^2(\overline{n}_h - \overline{n}_c)}{\Gamma\Phi + 4g^2|\mathcal{E}|^2\Psi} - \frac{\kappa}{2}\right]\mathcal{E} = \frac{1}{2}\left[\frac{G}{1 + B|\mathcal{E}|^2} - \kappa\right]\mathcal{E}. \qquad (8)$$

In the above bracket, $G := 4g^2\Delta N_0/\Gamma$ is the lasing gain and $G/\kappa \geqslant 1$ means above the lasing threshold; $B := 4g^2\Psi/\Gamma\Phi$ is the saturation parameter. It is worth noticing that, although the population inversion ΔN_0 increases with $\overline{n}_h$, it also gets saturated and could never exceed 1, while the atomic decay rate Γ keeps increasing linearly with $\overline{n}_h$.

As a result, with increasing T_h starting from T_c, the lasing gain first increases from zero and gets above the threshold, but then the lasing gain achieves a maximum point, after which it starts to decrease, and even goes below the threshold again at a very high temperature T_h [Figs. 2(a) and 2(b)]. Intuitively, a higher T_h would enhance the population inversion for lasing; however, a higher T_h also enhances the atomic decay rate Γ, which suppresses the lasing gain [Eq. (8)]. Therefore, at a very high temperature T_h, the lasing gain decreases and even below the threshold again.

In Fig. 2(b) we show a numerical result for the atomic populations in the steady state changing with T_h. When T_h is very high, the populations on $|e_{1,2}\rangle$ are almost totally inverted, but the lasing gain G decreases with T_h. In addition, the cavity photon number $\langle\hat{n}_l\rangle$ shows similar behavior [Fig. 2(c)]. Notice that the photon number $\langle\hat{n}_l\rangle$ in the cavity is not large; this is because we have only one atom in the cavity and thus the photon emission is limited.

If the cavity coupling strength g is strong or atomic spontaneous decay rates $\gamma_{h,c}$ are weak, the second critical point would appear at a much higher temperature T_h, but such a behavior of double critical points always exists. For realistic laser systems with N atoms in the cavity, the coupling strength could be effectively enhanced by the atom number ($\sqrt{N}g$). Therefore, it is not easy to observe such double-threshold behavior in common laser systems since the second threshold is usually too high and beyond the practical regime of interest. However, for a single-atom heat engine laser, it is much easier for this double-threshold behavior to happen. In the finite
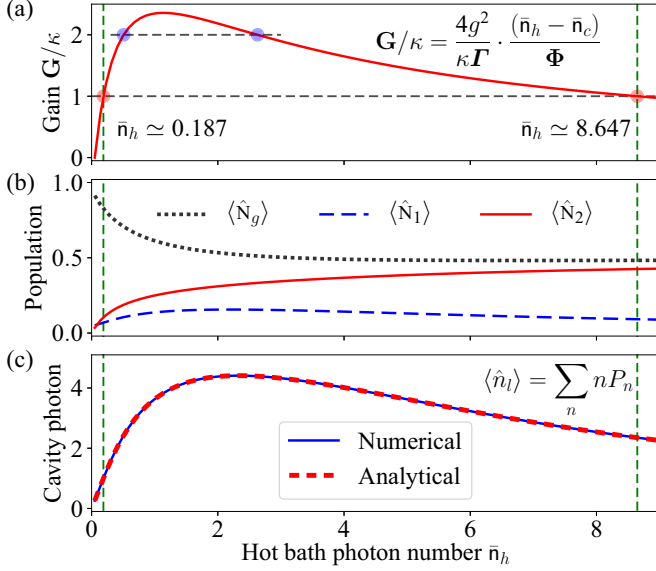
FIG. 2. (a) Lasing gain G. Here $G/\kappa \geqslant 1$ means above the lasing threshold. (b) Steady-state populations on $|g\rangle$, $|e_{1,2}\rangle$. (c) Average photon number $\langle \hat{n}_l \rangle$ in the cavity obtained from the analytical result (13) and (17) (red dashed line) and numerically solving the master equation directly (blue solid line). We set $\gamma_h = \gamma_c = 32\kappa$, $g = 14\kappa$, and $\bar{n}_c = 0.05$ as the cold bath photon number. The two critical points are $\bar{n}_h \simeq 0.187$ and $\bar{n}_h \simeq 8.647$.

cavity limit $\kappa \to 0$, this threshold condition simply reduces as $\bar{n}_h - \bar{n}_c \geqslant 0$ and then it leads to the SSDB inequality $\eta_{\text{SSDB}} = \Omega_l/\omega_h \leqslant 1 - T_c/T_h$, which was derived based on the comparison of the Boltzmann factors [1].

III. FULLY QUANTUM APPROACH

The semiclassical approach is helpful to get a basic understanding of the physical process in this heat engine. To get a more precise and rigorous description, we adopt the Scully-Lamb approach to study the fully quantum theory for the cavity mode $\varrho := \text{tr}_{\text{atom}}\rho$ [23–25,27]. In this approach, the previous semiclassical separation of the correlation functions are not needed. Defining the matrix elements of ϱ in Fock basis as $P_{mn} := \langle m|\varrho|n\rangle$, we have

$$\frac{d}{dt}P_{mn} = ig(\sqrt{n}\rho_{12;m,n-1} - \sqrt{m}\rho_{21;m-1,n})$$
$$- ig(\sqrt{m+1}\rho_{12;m+1,n} - \sqrt{n+1}\rho_{21;m,n+1})$$
$$+ \kappa[\sqrt{(m+1)(n+1)}P_{m+1,n+1} - \tfrac{1}{2}(m+n)P_{mn}].$$
$$(9)$$

Here $\rho_{\alpha\beta;mn} := \langle \alpha,m|\rho|\beta,n\rangle$ and $\alpha,\beta = 1,2,g$ are the atom state indices. The first two terms mean that the dynamics of the cavity mode and the atom are coupled together and we need to eliminate the atom degree of freedom.

For this purpose, we adopt the adiabatic elimination to take away the dynamics of the atom [23–25]. Namely, we assume that the atom decays very fast and quickly arrives at its steady state ($\kappa \ll \gamma_{h,c}$). That gives a set of algebraic equations, which enable us to obtain the equation for the photon number

probability $P_n := \langle n|\varrho|n\rangle$ (see Appendix A),

$$\frac{d}{dt}P_n = \frac{n[\mathscr{A}P_{n-1} - \mathscr{A}_b P_n]}{1 + n\mathscr{B}/\mathscr{A}} - \frac{(n+1)[\mathscr{A}P_n - \mathscr{A}_b P_{n+1}]}{1 + (n+1)\mathscr{B}/\mathscr{A}}$$
$$+ \kappa[(n+1)P_{n+1} - nP_n],$$
$$(10)$$

where we define

$$\mathscr{A} := \frac{4g^2\bar{n}_h(\bar{n}_c + 1)}{\Gamma\Phi}, \quad \mathscr{A}_b = \frac{4g^2\bar{n}_c(\bar{n}_h + 1)}{\Gamma\Phi},$$
$$\mathscr{B} := \mathscr{A}\frac{4g^2\Psi}{\Gamma\Phi}.$$
$$(11)$$

The constants Γ, Φ, and Ψ are the same as in Eqs. (4) and (5). This equation has the same form as in Ref. [27] [p. 297, Eq. (59)]. Here $\mathscr{A}$ indicates the stimulated emission rate, while $\mathscr{A}_b$ is the stimulated absorption rate.

Expending the fractions in the above lasing equation to first order, we further derive the equation for the average photon number $\langle \hat{n}_l \rangle = \sum nP_n$, i.e.,

$$\frac{d}{dt}\langle \hat{n}_l \rangle = (\mathscr{A} - \mathscr{A}_b - \kappa)\langle \hat{n}_l \rangle + \mathscr{A} - \mathscr{B}\langle (\hat{n}_l + 1)^2 \rangle$$
$$+ \frac{\mathscr{A}}{\mathscr{A}_b}\mathscr{B}\langle \hat{n}_l^2 \rangle \cdots .$$
$$(12)$$

The first linear term is the net lasing gain, which is exactly the same as that in the previous semiclassical laser equation (8), and we can verify $\mathscr{A} - \mathscr{A}_b = G$. The $\mathscr{B}$ terms are nonlinear saturation which is beyond the linearized laser theory.

IV. PHOTON NUMBER STATISTICS

Setting $\dot{P}_n = 0$ in the lasing equation (10), the photon number distribution of the cavity mode in the steady state is obtained as follows:

$$\frac{P_n}{P_{n-1}} = \frac{\mathscr{A}}{\mathscr{A}_b + \kappa\left(1 + \frac{n\mathscr{B}}{\mathscr{A}}\right)},$$
$$P_n = P_0 \prod_{k=1}^{n} \frac{\mathscr{A}}{\mathscr{A}_b + \kappa\left(1 + \frac{k\mathscr{B}}{\mathscr{A}}\right)} \quad (n \geqslant 1).$$
$$(13)$$

The maximum probability of P_n appears around

$$n_* = \frac{\mathscr{A}}{\kappa\mathscr{B}}(\mathscr{A} - \mathscr{A}_b - \kappa).$$
$$(14)$$

Here P_n increases when $n < n_*$ but decreases when $n > n_*$. Thus the lasing threshold requires $n_* \geqslant 0$, which is just the same as the above-threshold condition $G - \kappa = \mathscr{A} - \mathscr{A}_b - \kappa \geqslant 0$.

When the system is working far below the threshold, approximately the distribution becomes an exponentially decaying one,

$$\frac{P_n}{P_{n-1}} = \frac{\mathscr{A}}{\mathscr{A}_b + \kappa} \leqslant 1.$$
$$(15)$$

Therefore, the output light is like thermal radiation. However, we should recall that if the system is below but still close to the lasing threshold, the the realistic photon distribution is not the idealistic thermal one [Eq. (13)]. For example, Figs. 3(b) and 3(c) show that P_n is not exactly an exponentially decaying
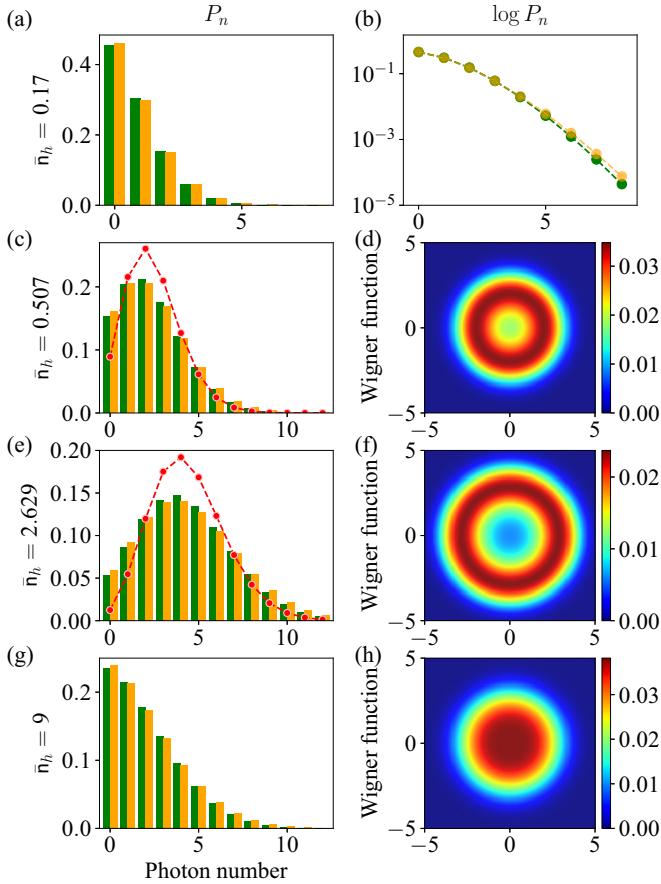
FIG. 3. Photon number distributions and Wigner functions. The parameters are the same as those in Fig. 2 and (a) and (b) $\bar{n}_h = 0.17$ (below threshold), (c) and (d) $\bar{n}_h = 0.507$ (above threshold), (e) and (f) $\bar{n}_h = 2.629$ (above threshold), and (g) and (h) $\bar{n}_h = 9$ (below threshold). Notice that $\bar{n}_h = 0.507$ in (c) and (d) and $\bar{n}_h = 2.629$ in (e) and (f) are the two blue points in Fig. 2(a) which have the same gain $G/\kappa = 2$. The two critical points are $\bar{n}_h \simeq 0.187$ and $\bar{n}_h \simeq 8.647$. The yellow columns (right) are given by the analytical result (13) and the green columns (left) are the numerical result by solving the master equation (1) directly. The distributions below the lasing threshold in (a), (b), (g), and (h) are not exactly thermal distributions ($P_n \propto \exp[-n\Omega_l/T]$). The red dashed lines in (c) and (e) are the corresponding Poisson distribution $P_n = e^{-\langle \hat{n}_l \rangle} \langle \hat{n}_l \rangle^n / n!$, where $\langle \hat{n}_l \rangle$ is the average photon number.

distribution. In addition, above the threshold, the distribution is not the perfect Poisson one either [24,25].

In Fig. 3 we show the photon number distributions and the corresponding Wigner functions when T_h is in different regimes. The photon number distribution is calculated by the above analytical result (13) (yellow columns on the right) as well as by solving the master equation (1) numerically (green columns on the left), and they match each other quite well for all different T_h, which confirms the validity of the above adiabatic elimination method. Further, it shows that with increasing T_h, the cavity output light first gives out thermal light, then becomes lasing, and then turns back to be thermal again in the very-high-temperature regime, which confirms our previous result.

It is worth noticing that the two blue points in Fig. 2(a) ($\bar{n}_h \simeq 0.507$ and $\bar{n}_h \simeq 2.629$) have the same gain G, but their distributions still differ greatly [see Figs. 3(c) and 3(e)]. For example, their maximum value also depends on $\mathscr{A}/\mathscr{B}$ [see Eq. (14)].

The total output power of the cavity is

$$\mathcal{P}_l = -\text{tr}(\mathcal{L}_{\text{cav}}[\rho]\hbar\Omega_l\hat{n}_l) = \hbar\Omega_l\kappa\langle\hat{n}_l\rangle, \qquad (16)$$

which is proportional to the average photon number of the cavity mode. From the photon number distribution (13), we obtain the average photon number (see Appendix A)

$$\langle\hat{n}_l\rangle = \frac{\mathscr{A}}{\kappa\mathscr{B}}(\mathscr{A} - \mathscr{A}_\flat - \kappa) + \frac{\mathscr{A}}{\kappa\mathscr{B}}(\kappa + \mathscr{A}_\flat)P_0. \qquad (17)$$

In Fig. 2(c) we compare this analytical result for cavity photon number with the numerical result by solving the master equation (1) directly; they fit each other quite well.

When the system is far above the threshold, $P_0 \simeq 0$ and thus only the first term dominates. Therefore, the laser power is

$$\mathcal{P}_l = \hbar\Omega_l\frac{\mathscr{A}}{\mathscr{B}}(\mathscr{A} - \mathscr{A}_\flat - \kappa)$$

$$= \frac{\hbar\Omega_l\gamma_h\gamma_c(\bar{n}_h - \bar{n}_c - \frac{\kappa}{4g^2}\Gamma\Phi)}{\gamma_h(3\bar{n}_h + 1) + \gamma_c(3\bar{n}_c + 1)}. \qquad (18)$$

The leading term of this result (without the κ term) is the same as that in Ref. [9], which was calculated by rate equations (see Eq. [S6] in the Supplemental Material thereof). This result is valid when the system is far above the lasing threshold. When the system is below or around the threshold, the P_0 term in Eq. (17) becomes important and cannot be neglected [Fig. 2(c)]. Considering $\bar{n}_c \sim 0$ and $\gamma_h = \gamma_c = \gamma$, a rough estimation for the cavity photon number is

$$\langle\hat{n}_l\rangle \sim \frac{\gamma\bar{n}_h}{\kappa(3\bar{n}_h + 2)} - \frac{\gamma^2}{4g^2}\frac{(\bar{n}_h + 1)(2\bar{n}_h + 1)}{3\bar{n}_h + 2}, \qquad (19)$$

where the second term increases with $\bar{n}_h$ monotonically and indicates that the hot photon number could weaken the lasing. Thus the maximum cavity photon number does not appear at $\bar{n}_h \to \infty$. Again we see that the cavity photon number is not large, which is because there is only one single atom in the cavity and thus the photon emission is limited.

Further, with this distribution P_n, the variance of the photon number is

$$\sigma^2 := \langle\hat{n}_l^2\rangle - \langle\hat{n}_l\rangle^2 = \frac{\mathscr{A}^2}{\kappa\mathscr{B}} - \frac{\mathscr{A}}{\kappa\mathscr{B}}(\kappa + \mathscr{A}_\flat)P_0\langle\hat{n}_l\rangle. \qquad (20)$$

When the system is far above the threshold, $P_0 \simeq 0$ and

$$\frac{\sigma^2}{\langle\hat{n}_l\rangle} = 1 + \frac{\mathscr{A}_\flat + \kappa}{\mathscr{A} - \mathscr{A}_\flat - \kappa}. \qquad (21)$$

Thus the lasing photon number distribution is super-Poissonian ($\sigma^2 > \langle\hat{n}_l\rangle$). When $\mathscr{A} \gg \mathscr{A}_\flat + \kappa$, the photon distribution approaches the Poissonian one with $\sigma^2 \simeq \langle\hat{n}_l\rangle$.

V. FOUR-LEVEL HEAT ENGINE MODEL

In the above discussion, we notice that the three-level heat engine has a problem of double critical points, namely, when
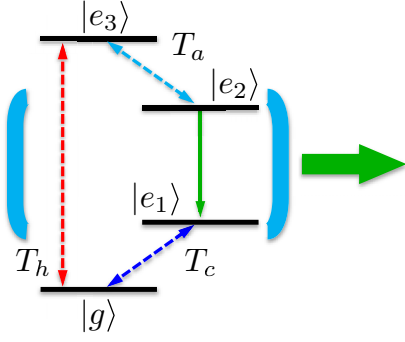
FIG. 4. Four-level heat engine. The transition $|e_2\rangle \leftrightarrow |e_3\rangle$ is coupled with a third ancilla bath with temperature T_a.

the hot bath temperature is increased, the atomic coherence decay rate is also increased, which decreases the lasing gain and even below the threshold again. To avoid this problem, we consider a four-level system as shown in Fig. 4 [26]. The transition $|e_2\rangle \leftrightarrow |e_3\rangle$ is coupled with a third ancilla bath with a low temperature T_a so as to "cool down" the atomic coherence decay rate of the lasing transition. In addition, this third bath also increases the population on $|e_2\rangle$, as we will show below.

Using the same method as the above discussion (see also Appendix B), the linearized semiclassical lasing equation is

$$\dot{\mathcal{E}} \simeq \frac{1}{2}\left[\frac{4g^2}{\Gamma'}\Delta N_0' - \kappa\right]\mathcal{E} + o(|\mathcal{E}|^2),$$

$$\Delta N_0' = [(\bar{n}_h - \bar{n}_c)\bar{n}_a + (\bar{n}_c + 1)\bar{n}_h]/\Phi', \qquad (22)$$

where $G' := 4g^2\Delta N_0'/\Gamma'$ is the lasing gain and

$$\Gamma' = \gamma_a\bar{n}_a + \gamma_c(\bar{n}_c + 1),$$
$$\Phi' = (4\bar{n}_h\bar{n}_c + 3\bar{n}_h + 2\bar{n}_c + 1)\bar{n}_a + \bar{n}_h(\bar{n}_c + 1). \qquad (23)$$

Here $\bar{n}_a := \bar{n}_P(\omega_a, T_a)$ is the thermal photon number of the transition $|e_2\rangle \leftrightarrow |e_3\rangle$ and $\omega_a = E_3 - E_2$. In this case, the decay rate Γ' does not depend on the hot bath and thus will not increase with T_h as the three-level case. In addition, it is clear to see that $G'/\kappa = 1$ is a linear equation and gives only one root for $\bar{n}_h$ when $\bar{n}_{c,a}$ are fixed, which means that only one critical point exists (see Fig. 5).

Simple algebra shows that $\Delta N_0'$ is the population inversion on $|e_2\rangle$ and $|e_1\rangle$ when there is no cavity coupling. Notice that when $T_a \to 0$, we have $\Delta N_0' \to 1$, which means that all the populations would fall on $|e_2\rangle$ in the steady state. This is because when $T_a = 0$, once the population falls down from $|e_3\rangle$ to $|e_2\rangle$, it could never go back. This is the maximum inversion for lasing. In Fig. 5 we also notice that the lasing threshold is much easier to achieve than in the three-level case, i.e., a very small $\bar{n}_h$ provides a strong enough pumping for lasing.

In the finite cavity limit $\kappa \to 0$, the lasing condition is given by $\Delta N_0' \geqslant 0$ [Eq. (22)], which leads to

$$e^{\omega_a/T_a}e^{\omega_c/T_c} \geqslant e^{\omega_h/T_h}. \qquad (24)$$

If we consider that the ancilla bath has the same temperature as the cold one, $T_a = T_c$, the above inequality gives

$$1 - \frac{T_c}{T_h} \geqslant 1 - \frac{\omega_a + \omega_c}{\omega_h} = \frac{\Omega_l}{\omega_h}. \qquad (25)$$
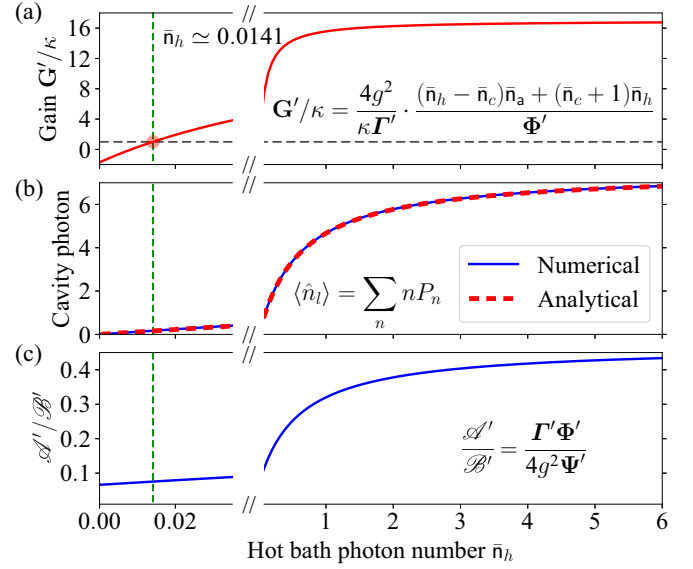

FIG. 5. (a) Lasing gain G' for the four-level system. (b) Average photon number $\langle\hat{n}_l\rangle$ in the cavity obtained from the analytical result (red dashed line) and numerically solving the master equation directly (blue solid line). (c) Ratio $\mathscr{A}'/\mathscr{B}'$. We set $\gamma_h = \gamma_c = \gamma_a = 32\kappa$, $g = 14\kappa$, $\bar{n}_c = 0.1$, and $\bar{n}_a = 0.1$. The critical point is $\bar{n}_h \simeq 0.0141$.

Here Ω_l/ω_h is just the output efficiency of this four-level system and again it is bounded by the Carnot efficiency, which is similar to the previous SSDB discussion.

The fully quantum equation also has the same form as the three-level case [Eq. (10)], except that the parameters $\mathscr{A}$, $\mathscr{A}_b$, and $\mathscr{B}$ should be changed to be (see Appendix B)

$$\mathscr{A}' := \frac{4g^2\bar{n}_h(\bar{n}_c + 1)(\bar{n}_a + 1)}{\Gamma'\Phi'}, \quad \mathscr{A}_b' = \frac{4g^2\bar{n}_c\bar{n}_a(\bar{n}_h + 1)}{\Gamma'\Phi'},$$

$$\mathscr{B}' := \mathscr{A}'\frac{4g^2\Psi'}{\Gamma'\Phi'}, \qquad (26)$$

where $\Psi' = \gamma_h^{-1}(4\bar{n}_a\bar{n}_c + \bar{n}_a + 3\bar{n}_c + 1) + \gamma_c^{-1}(4\bar{n}_h\bar{n}_a + 2\bar{n}_h + \bar{n}_a) + \gamma_a^{-1}(4\bar{n}_h\bar{n}_c + 2\bar{n}_h + 3\bar{n}_c + 1)$. In Fig. 5 we show the lasing gain and the cavity photon number, which increase monotonically with the hot bath temperature T_h. Again, the laser gain is just given by $G' = \mathscr{A}' - \mathscr{A}_b'$.

The cavity photon number is still given by Eq. (17), but the parameters should be changed by $\mathscr{A}'$, $\mathscr{A}_b'$, and $\mathscr{B}'$, correspondingly. Figure 5(c) shows that this analytical result for the cavity photon number fits quite well with the numerical result.

When the system is far above threshold, the laser power is estimated by (considering $\kappa \to 0$)

$$\kappa\langle\hat{n}_l\rangle \simeq \frac{G'\mathscr{A}'}{\mathscr{B}'} = [(\bar{n}_h - \bar{n}_c)\bar{n}_a + (\bar{n}_c + 1)\bar{n}_h]/\Psi'. \qquad (27)$$

If we further consider $\bar{n}_{c,a} \sim 0$, $\gamma_h = \gamma_c = \gamma_a = \gamma$, and $\bar{n}_h \gg 1$, then the maximum gain and cavity photon number are around $G' \sim 4g^2/\gamma$ and $\langle\hat{n}_l\rangle \sim \gamma/4\kappa$. Both the lasing gain G' and the cavity photon number $\langle\hat{n}_l\rangle$ approach saturation in the very-high-temperature regime, as shown in Fig. 5. This is because in this regime, the population is almost totally inverted ($\Delta N_0' \to 1$) and thus the increase of the hot bath temperature

T_h can no longer cause a significant increase of the lasing gain. Unlike the three-level result (19), the hot bath no longer has any weakening effect on the lasing and thus more lasing photons can be produced in the cavity, and the lasing power can be increased. However, the cavity photon number is still limited due to the single-atom feature.

VI. SUMMARY

In this paper we studied the statistics of the lasing output from the SSDB heat engine. In this heat engine model, a single three-level atom is coupled with the quantized cavity mode and is in contact with a hot and a cold heat bath together. We derived a laser equation for this heat engine model and obtained the photon number distribution both below and above the lasing threshold. Below the lasing threshold, the output light from the cavity is more likely thermal radiation. With the increase of the hot bath temperature, the population is inverted and lasing light comes out. If the hot bath temperature keeps increasing, our analytical result shows that the atomic decay rate is also

enhanced, which weakens the lasing gain. As a result, at a very high temperature of the hot bath, another critical point appears and after that the output light becomes thermal radiation again.

To avoid this double-threshold behavior, we considered a four-level model where neither of the two lasing levels is coupled with the hot bath directly and a third ancilla bath is introduced. As a result, the atomic decay rate in this four-level no longer depends on the hot bath temperature and thus the lasing gain and cavity photon number keep increasing monotonically when the hot bath temperature increases. This four-level heat engine is also bounded by the Carnot efficiency, which is the same as the original three-level SSDB model.

APPENDIX A: LASING EQUATION FOR THE THREE-LEVEL SYSTEM

1. Lasing equation

Here we derive the lasing equation for the photon number distribution $P_n = \langle n|\varrho|n \rangle$, where $\varrho = \mathrm{tr}_{\mathrm{atom}}\rho$ is the density matrix of the cavity mode. We assume that the cavity leaking is much slower than the atom decay and omit $\mathcal{L}_{\mathrm{cav}}[\rho]$; then the master equation (1) gives (defining $\rho_{\alpha\beta;mn} = \langle \alpha,m|\rho|\beta,n \rangle$, where $\alpha,\beta = 1,2,g$ are the atom state indices)

$$\frac{d}{dt}\rho_{11;mn} = ig(\sqrt{n}\rho_{12;m,n-1} - \sqrt{m}\rho_{21;m-1,n}) - \Gamma_c^-\rho_{11;mn} + \Gamma_c^+\rho_{gg;mn},$$

$$\frac{d}{dt}\rho_{22;mn} = ig(\sqrt{n+1}\rho_{21;m,n+1} - \sqrt{m+1}\rho_{12;m+1,n}) - \Gamma_h^-\rho_{22;mn} + \Gamma_h^+\rho_{gg;mn},$$

$$\frac{d}{dt}\rho_{12;mn} = ig(\sqrt{n+1}\rho_{11;m,n+1} - \sqrt{m}\rho_{22;m-1,n}) - \frac{1}{2}(\Gamma_h^- + \Gamma_c^-)\rho_{12;mn},$$

$$\frac{d}{dt}\rho_{21;mn} = -ig(\sqrt{m+1}\rho_{11;m+1,n} - \sqrt{n}\rho_{22;m,n-1}) - \frac{1}{2}(\Gamma_h^- + \Gamma_c^-)\rho_{21;mn},$$

$$\frac{d}{dt}\rho_{gg;mn} = \Gamma_c^-\rho_{11;mn} - \Gamma_c^+\rho_{gg;mn} + \Gamma_h^-\rho_{22;mn} - \Gamma_h^+\rho_{gg;mn}. \tag{A1}$$

Here we define $\Gamma_i^+ = \gamma_i\bar{n}_i$ and $\Gamma_i^- = \gamma_i(\bar{n}_i + 1)$ for $i = h,c$. The matrix elements for the cavity mode is $P_{mn} := \langle m|\varrho|n \rangle = \rho_{11;mn} + \rho_{22;mn} + \rho_{gg;mn}$; thus, combined with the cavity leaking term $\mathcal{L}_{\mathrm{cav}}[\rho]$, the equation for the cavity mode is

$$\frac{d}{dt}P_{mn} = ig(\sqrt{n}\rho_{12;m,n-1} - \sqrt{m}\rho_{21;m-1,n}) - ig(\sqrt{m+1}\rho_{12;m+1,n} - \sqrt{n+1}\rho_{21;m,n+1})$$

$$+ \kappa[\sqrt{(m+1)(n+1)}P_{m+1,n+1} - \frac{1}{2}(m+n)P_{mn}]. \tag{A2}$$

In the first two terms, the dynamics of the cavity mode is still coupled with that of the atom.

To derive a equation for the cavity mode alone, we need to replace $\rho_{12;mn}$ by P_{mn} in Eqs. (A2) by adiabatic elimination [24,25]. That is, due to the fast decay of the atom, Eqs. (A1) quickly arrive at the steady state, which gives

$$0 = ig(\sqrt{n}\rho_{12;m,n-1} - \sqrt{m}\rho_{21;m-1,n}) - \Gamma_c^-\rho_{11;mn} + \Gamma_c^+\rho_{gg;mn},$$

$$0 = ig(\sqrt{n}\rho_{21;m-1,n} - \sqrt{m}\rho_{12;m,n-1}) - \Gamma_h^-\rho_{22;m-1,n-1} + \Gamma_h^+\rho_{gg;m-1,n-1},$$

$$0 = ig(\sqrt{n}\rho_{11;mn} - \sqrt{m}\rho_{22;m-1,n-1}) - \frac{1}{2}(\Gamma_h^- + \Gamma_c^-)\rho_{12;m,n-1},$$

$$0 = -ig(\sqrt{m}\rho_{11;mn} - \sqrt{n}\rho_{22;m-1,n-1}) - \frac{1}{2}(\Gamma_h^- + \Gamma_c^-)\rho_{21;m-1,n},$$

$$0 = \Gamma_c^-\rho_{11;mn} - \Gamma_c^+\rho_{gg;mn} + \Gamma_h^-\rho_{22;mn} - \Gamma_h^+\rho_{gg;mn},$$

$$0 = \Gamma_c^-\rho_{11;m-1,n-1} - \Gamma_c^+\rho_{gg;m-1,n-1} + \Gamma_h^-\rho_{22;m-1,n-1} - \Gamma_h^+\rho_{gg;m-1,n-1}. \tag{A3}$$

Together with the relations

$$P_{mn} = \rho_{11;mn} + \rho_{22;mn} + \rho_{gg;mn},$$

$$P_{m-1,n-1} = \rho_{11;m-1,n-1} + \rho_{22;m-1,n-1} + \rho_{gg;m-1,n-1}, \tag{A4}$$

Eqs. (A3) and (A4) become a closed set for the eight variables $\rho_{gg;mn}$, $\rho_{11;mn}$, $\rho_{22;mn}$, $\rho_{gg;m-1,n-1}$, $\rho_{11;m-1,n-1}$, $\rho_{22;m-1,n-1}$, $\rho_{12;m,n-1}$, and $\rho_{21;m-1,n}$. Solving this equation set, we obtain the steady values of $\rho_{12;mn}$ represented by P_{mn}. Here we are concerned with only the diagonal terms $P_n = \langle n|\varrho|n\rangle$ $(m = n)$, which gives

$$ig(\sqrt{n}\rho_{12;n,n-1} - \sqrt{n}\rho_{21;n-1,n}) = \frac{n[4g^2\overline{\mathrm{n}}_h(\overline{\mathrm{n}}_c + 1)P_{n-1} - 4g^2\overline{\mathrm{n}}_c(\overline{\mathrm{n}}_h + 1)P_n]}{\Gamma\Phi + n4g^2\Psi} \tag{A5}$$

for the first two terms in Eqs. (A2), where

$$\Gamma := \gamma_c(\overline{\mathrm{n}}_c + 1) + \gamma_h(\overline{\mathrm{n}}_h + 1), \quad \Phi = 3\overline{\mathrm{n}}_h\overline{\mathrm{n}}_c + 2(\overline{\mathrm{n}}_h + \overline{\mathrm{n}}_c) + 1, \quad \Psi := \frac{1}{\gamma_h\gamma_c}[\gamma_h(3\overline{\mathrm{n}}_h + 1) + \gamma_c(3\overline{\mathrm{n}}_c + 1)], \tag{A6}$$

Then we obtain the lasing equation for the cavity mode [see Ref. [27], p. 297, Eq. (59)]

$$\frac{d}{dt}P_n = \frac{n[\mathscr{A}P_{n-1} - \mathscr{A}_{\mathrm{b}}P_n]}{1 + n\mathscr{B}/\mathscr{A}} - \frac{(n+1)[\mathscr{A}P_n - \mathscr{A}_{\mathrm{b}}P_{n+1}]}{1 + (n+1)\mathscr{B}/\mathscr{A}} + \kappa[(n+1)P_{n+1} - nP_n], \tag{A7}$$

where we define

$$\mathscr{A} := \frac{4g^2\overline{\mathrm{n}}_h(\overline{\mathrm{n}}_c + 1)}{\Gamma\Phi}, \quad \mathscr{A}_{\mathrm{b}} := \frac{4g^2\overline{\mathrm{n}}_c(\overline{\mathrm{n}}_h + 1)}{\Gamma\Phi}, \quad \mathscr{B} := \mathscr{A}\frac{4g^2\Psi}{\Gamma\Phi}. \tag{A8}$$

2. Photon number statistics

In Eq. (A7) of $\dot{P}_n$, expanding the fractions to first order, the average photon number $\langle \hat{n}_l \rangle = \sum n P_n$ gives

$$\frac{d}{dt}\langle \hat{n}_l \rangle = (\mathscr{A} - \mathscr{A}_{\mathrm{b}} - \kappa)\langle \hat{n}_l \rangle + \mathscr{A} - \mathscr{B}\langle(\hat{n}_l + 1)^2\rangle + \frac{\mathscr{A}}{\mathscr{A}_{\mathrm{b}}}\mathscr{B}\langle\hat{n}_l^2\rangle + \cdots . \tag{A9}$$

In the steady state, the photon number distribution is

$$\frac{P_n}{P_{n-1}} = \frac{\mathscr{A}}{\mathscr{A}_{\mathrm{b}} + \kappa\left(1 + \frac{n\mathscr{B}}{\mathscr{A}}\right)}, \quad P_n = P_0 \prod_{k=1}^{n} \frac{(\mathscr{A}^2/\kappa\mathscr{B})}{\frac{\mathscr{A}}{\kappa\mathscr{B}}(\kappa + \mathscr{A}_{\mathrm{b}}) + k} := \frac{P_0 Y! X^n}{(n + Y)!}, \tag{A10}$$

where we define $X := \mathscr{A}^2/\kappa\mathscr{B}$ and $Y := \frac{\mathscr{A}}{\kappa\mathscr{B}}(\kappa + \mathscr{A}_{\mathrm{b}})$. The average photon number is

$$\langle \hat{n}_l \rangle = \sum_{n=0}^{\infty} n\frac{P_0 Y! X^n}{(n + Y)!} = P_0 Y! \sum_{n=1}^{\infty} \frac{(n + Y - Y)X^n}{(n + Y)!} = P_0 Y! \sum_{n=1}^{\infty} \left[\frac{X X^{n-1}}{(n - 1 + Y)!} - \frac{Y X^n}{(n + Y)!}\right]$$

$$= X - Y + Y P_0 = \frac{\mathscr{A}}{\kappa\mathscr{B}}(\mathscr{A} - \mathscr{A}_{\mathrm{b}} - \kappa) + \frac{\mathscr{A}}{\kappa\mathscr{B}}(\kappa + \mathscr{A}_{\mathrm{b}})P_0. \tag{A11}$$

When the system is far above the threshold, $P_0 \simeq 0$ and then we obtain

$$\kappa\langle \hat{n}_l \rangle = \frac{\mathscr{A}}{\mathscr{B}}(\mathscr{A} - \mathscr{A}_{\mathrm{b}} - \kappa) = \frac{\gamma_h\gamma_c(\overline{\mathrm{n}}_h - \overline{\mathrm{n}}_c - \frac{\kappa}{4g^2}\Gamma\Phi)}{\gamma_h(3\overline{\mathrm{n}}_h + 1) + \gamma_c(3\overline{\mathrm{n}}_c + 1)}. \tag{A12}$$

Notice that the radiation power of the cavity is just $\mathcal{P}_l = -\hbar\Omega_l\frac{d}{dt}\langle \hat{n}_l \rangle|_{\mathrm{cav}} = \hbar\Omega_l\kappa\langle \hat{n}_l \rangle$. The leading term of this result is consistent with that in Ref. [9].

The variance of the photon number distribution is calculated by

$$\langle\hat{n}_l^2\rangle = \sum_{n=0}^{\infty} n^2\frac{P_0 Y! X^n}{(n + Y)!} = P_0 Y! \sum_{n=1}^{\infty} \left[\frac{n X X^{n-1}}{(n - 1 + Y)!} - \frac{n Y X^n}{(n + Y)!}\right]$$

$$= \sum_{n=0}^{\infty}(n + 1)X\frac{P_0 Y! X^n}{(n + Y)!} - n Y\frac{P_0 Y! X^n}{(n + Y)!} = \langle\hat{n}_l + 1\rangle X - \langle\hat{n}_l\rangle Y,$$

$$\sigma^2 := \langle\hat{n}_l^2\rangle - \langle\hat{n}_l\rangle^2 = X - Y P_0(X - Y + Y P_0) = \frac{\mathscr{A}^2}{\kappa\mathscr{B}} - \frac{\mathscr{A}}{\kappa\mathscr{B}}(\kappa + \mathscr{A}_{\mathrm{b}})P_0\langle\hat{n}_l\rangle. \tag{A13}$$

When the system is far above the threshold, $P_0 \simeq 0$ and we have

$$\sigma^2 = \frac{\mathscr{A}^2}{\kappa\mathscr{B}} = \langle\hat{n}_l\rangle + \frac{\mathscr{A}}{\kappa\mathscr{B}}(\mathscr{A}_{\mathrm{b}} + \kappa), \qquad \frac{\sigma^2}{\langle\hat{n}_l\rangle} = 1 + \frac{\mathscr{A}_{\mathrm{b}} + \kappa}{\mathscr{A} - \mathscr{A}_{\mathrm{b}} - \kappa}. \tag{A14}$$

If we have $\mathscr{A} \gg \mathscr{A}_{\mathrm{b}} + \kappa$, the photon distribution approaches the Poisson one with $\sigma^2 \simeq \langle\hat{n}_l\rangle$.

APPENDIX B: LASING EQUATION FOR THE FOUR-LEVEL SYSTEM

1. Semiclassical lasing equation

Here we study the lasing equation for the four-level model shown in Fig. 4. First we consider the semiclassical equations similar to Eqs. (3). We have

$$\frac{d}{dt}\langle\hat{N}_1\rangle = \gamma_c[\bar{n}_c\langle\hat{N}_g\rangle - (\bar{n}_c + 1)\langle\hat{N}_1\rangle] - ig[\langle\hat{\sigma}^-\rangle\langle\hat{a}^\dagger\rangle - \langle\hat{\sigma}^+\rangle\langle\hat{a}\rangle],$$

$$\frac{d}{dt}\langle\hat{N}_2\rangle = -\gamma_a[\bar{n}_a\langle\hat{N}_2\rangle - (\bar{n}_a + 1)\langle\hat{N}_3\rangle] + ig[\langle\hat{\sigma}^-\rangle\langle\hat{a}^\dagger\rangle - \langle\hat{\sigma}^+\rangle\langle\hat{a}\rangle],$$

$$\frac{d}{dt}\langle\hat{N}_3\rangle = \gamma_h[\bar{n}_h\langle\hat{N}_g\rangle - (\bar{n}_h + 1)\langle\hat{N}_3\rangle] + \gamma_a[\bar{n}_a\langle\hat{N}_2\rangle - (\bar{n}_a + 1)\langle\hat{N}_3\rangle],$$

$$\frac{d}{dt}\langle\hat{\sigma}^-\rangle = ig\langle\hat{N}_2 - \hat{N}_1\rangle\langle\hat{a}\rangle - \frac{1}{2}\Gamma'\langle\hat{\sigma}^-\rangle,$$

$$\frac{d}{dt}\langle\hat{a}\rangle = -\frac{\kappa}{2}\langle\hat{a}\rangle - ig\langle\hat{\sigma}^-\rangle, \tag{B1}$$

where we define $\Gamma' = \gamma_a\bar{n}_a + \gamma_c(\bar{n}_c + 1)$ for the coherence decay rate. The steady state gives the population inversion as

$$\langle\hat{N}_2 - \hat{N}_1\rangle = \frac{(\bar{n}_h - \bar{n}_c)\bar{n}_a + (\bar{n}_c + 1)\bar{n}_h}{\Phi' + \frac{4g^2|\mathcal{E}|^2}{\Gamma'}\Psi'}, \tag{B2}$$

where

$$\Phi' = 4\bar{n}_a\bar{n}_h\bar{n}_c + 3\bar{n}_h\bar{n}_a + 2\bar{n}_a\bar{n}_c + \bar{n}_h\bar{n}_c + \bar{n}_h + \bar{n}_a,$$
$$\Psi' = \gamma_h^{-1}(4\bar{n}_a\bar{n}_c + \bar{n}_a + 3\bar{n}_c + 1) + \gamma_c^{-1}(4\bar{n}_h\bar{n}_a + 2\bar{n}_h + \bar{n}_a) + \gamma_a^{-1}(4\bar{n}_h\bar{n}_c + 2\bar{n}_h + 3\bar{n}_c + 1).$$

Therefore, the lasing equation is

$$\dot{\mathcal{E}} = \frac{2g^2}{\Gamma'}\langle\hat{N}_2 - \hat{N}_1\rangle\mathcal{E} - \frac{\kappa}{2}\mathcal{E} = \left[\frac{2g^2[(\bar{n}_h - \bar{n}_c)\bar{n}_a + (\bar{n}_c + 1)\bar{n}_h]}{\Gamma'\Phi' + 4g^2|\mathcal{E}|^2\Psi'} - \frac{\kappa}{2}\right]\mathcal{E}$$

$$\simeq \frac{1}{2}\left[\frac{4g^2[(\bar{n}_h - \bar{n}_c)\bar{n}_a + (\bar{n}_c + 1)\bar{n}_h]}{\Gamma'\Phi'} - \kappa\right]\mathcal{E}. \tag{B3}$$

2. Fully quantum approach

Now we consider the fully quantum approach. Similar to Eqs. (A1), the equations for the density elements are

$$\frac{d}{dt}\rho_{11;mn} = ig(\sqrt{n}\rho_{12;m,n-1} - \sqrt{m}\rho_{21;m-1,n}) - \Gamma_c^-\rho_{11;mn} + \Gamma_c^+\rho_{gg;mn},$$

$$\frac{d}{dt}\rho_{22;mn} = ig(\sqrt{n+1}\rho_{21;m,n+1} - \sqrt{m+1}\rho_{12;m+1,n}) - \Gamma_a^+\rho_{22;mn} + \Gamma_a^-\rho_{33;mn},$$

$$\frac{d}{dt}\rho_{12;mn} = ig(\sqrt{n+1}\rho_{11;m,n+1} - \sqrt{m}\rho_{22;m-1,n}) - \frac{1}{2}(\Gamma_a^+ + \Gamma_c^-)\rho_{12;mn},$$

$$\frac{d}{dt}\rho_{21;mn} = -ig(\sqrt{m+1}\rho_{11;m+1,n} - \sqrt{n}\rho_{22;m,n-1}) - \frac{1}{2}(\Gamma_a^+ + \Gamma_c^-)\rho_{21;mn},$$

$$\frac{d}{dt}\rho_{gg;mn} = \Gamma_c^-\rho_{11;mn} - \Gamma_c^+\rho_{gg;mn} + \Gamma_h^-\rho_{33;mn} - \Gamma_h^+\rho_{gg;mn},$$

$$\frac{d}{dt}\rho_{33;mn} = \Gamma_a^+\rho_{22;mn} - \Gamma_a^-\rho_{33;mn} - \Gamma_h^-\rho_{33;mn} + \Gamma_h^+\rho_{gg;mn}. \tag{B4}$$

Here we define $\Gamma_i^+ = \gamma_i\bar{n}_i$ and $\Gamma_i^- = \gamma_i(\bar{n}_i + 1)$ for $i = h, c, a$. The equation for the cavity mode is

$$\frac{d}{dt}P_{mn} = ig(\sqrt{n}\rho_{12;m,n-1} - \sqrt{m}\rho_{21;m-1,n}) - ig(\sqrt{m+1}\rho_{12;m+1,n} - \sqrt{n+1}\rho_{21;m,n+1})$$

$$+ \kappa[\sqrt{(m+1)(n+1)}P_{m+1,n+1} - \tfrac{1}{2}(m+n)P_{mn}]. \tag{B5}$$

The first two terms mean that the cavity mode is coupled with the atom.

We apply the adiabatic elimination and consider the steady state of the atom

$$
\begin{aligned}
0 &= ig(\sqrt{n}\,\rho_{12;m,n-1} - \sqrt{m}\,\rho_{21;m-1,n}) - \Gamma_c^-\rho_{11;mn} + \Gamma_c^+\rho_{gg;mn}, \\
0 &= ig(\sqrt{n}\,\rho_{21;m-1,n} - \sqrt{m}\,\rho_{12;m,n-1}) - \Gamma_a^+\rho_{22;m-1,n-1} + \Gamma_a^-\rho_{33;m-1,n-1}, \\
0 &= ig(\sqrt{n}\,\rho_{11;mn} - \sqrt{m}\,\rho_{22;m-1,n-1}) - \tfrac{1}{2}(\Gamma_a^+ + \Gamma_c^-)\rho_{12;m,n-1}, \\
0 &= -ig(\sqrt{m}\,\rho_{11;mn} - \sqrt{n}\,\rho_{22;m-1,n-1}) - \tfrac{1}{2}(\Gamma_a^+ + \Gamma_c^-)\rho_{21;m-1,n}, \\
0 &= \Gamma_c^-\rho_{11;mn} - \Gamma_c^+\rho_{gg;mn} + \Gamma_h^-\rho_{33;mn} - \Gamma_h^+\rho_{gg;mn}, \\
0 &= \Gamma_a^+\rho_{22;mn} - \Gamma_a^-\rho_{33;mn} - \Gamma_h^-\rho_{33;mn} + \Gamma_h^+\rho_{gg;mn}, \\
0 &= \Gamma_c^-\rho_{11;m-1,n-1} - \Gamma_c^+\rho_{gg;m-1,n-1} + \Gamma_h^-\rho_{33;m-1,n-1} - \Gamma_h^+\rho_{gg;m-1,n-1}, \\
0 &= \Gamma_a^+\rho_{22;m-1,n-1} - \Gamma_a^-\rho_{33;m-1,n-1} - \Gamma_h^-\rho_{33;m-1,n-1} + \Gamma_h^+\rho_{gg;m-1,n-1}.
\end{aligned}
\tag{B6}
$$

Together with the relations

$$
\begin{aligned}
P_{mn} &= \rho_{11;mn} + \rho_{22;mn} + \rho_{33;mn} + \rho_{gg;mn}, \\
P_{m-1,n-1} &= \rho_{11;m-1,n-1} + \rho_{22;m-1,n-1} + \rho_{33;m-1,n-1} + \rho_{gg;m-1,n-1},
\end{aligned}
\tag{B7}
$$

Eqs. (B6) and (B7) become a closed set for the ten variables $\rho_{gg;mn}$, $\rho_{11;mn}$, $\rho_{22;mn}$, $\rho_{33;mn}$, $\rho_{gg;m-1,n-1}$, $\rho_{11;m-1,n-1}$, $\rho_{22;m-1,n-1}$, $\rho_{33;m-1,n-1}$, $\rho_{12;m,n-1}$, and $\rho_{21;m-1,n}$. Solving this equation set, we obtain

$$
ig(\sqrt{n}\,\rho_{12;n,n-1} - \sqrt{n}\,\rho_{21;n-1,n}) = \frac{4g^2 n[\overline{n}_h(\overline{n}_c + 1)(\overline{n}_a + 1)P_{n-1} - \overline{n}_c\overline{n}_a(\overline{n}_h + 1)P_n]}{\Gamma'\Phi' + n4g^2\Psi'},
\tag{B8}
$$

where the parameters Γ', Φ', and Ψ' are just the same as those in the semiclassical results [Eqs. (B1) and (B2)]. Thus, the laser equation has the same form as the three-level case [Eqs. (10) and (A7)], except that the parameters $\mathscr{A}$, $\mathscr{A}_b$, and $\mathscr{B}$ are changed to

$$
\mathscr{A}' := \frac{4g^2\overline{n}_h(\overline{n}_c + 1)(\overline{n}_a + 1)}{\Gamma'\Phi'}, \quad
\mathscr{A}_b' = \frac{4g^2\overline{n}_c\overline{n}_a(\overline{n}_h + 1)}{\Gamma'\Phi'}, \quad
\mathscr{B}' := \mathscr{A}' \cdot \frac{4g^2\Psi'}{\Gamma'\Phi'}.
\tag{B9}
$$

[1] H. E. D. Scovil and E. O. Schulz-DuBois, Phys. Rev. Lett. **2**, 262 (1959).

[2] J. E. Geusic, E. O. Schulz-DuBois, and H. E. D. Scovil, Phys. Rev. **156**, 343 (1967).

[3] E. Geva and R. Kosloff, Phys. Rev. E **49**, 3903 (1994).

[4] N. Linden, S. Popescu, and P. Skrzypczyk, Phys. Rev. Lett. **105**, 130401 (2010).

[5] Y.-X. Chen and S.-W. Li, Europhys. Lett. **97**, 40003 (2012).

[6] R. Kosloff and Y. Rezek, Entropy **19**, 136 (2017).

[7] S. E. Harris, Phys. Rev. A **94**, 053859 (2016).

[8] Y. Zou, Y. Jiang, Y. Mei, X. Guo, and S. Du, Phys. Rev. Lett. **119**, 050602 (2017).

[9] M. O. Scully, K. R. Chapin, K. E. Dorfman, M. B. Kim, and A. Svidzinsky, Proc. Natl. Acad. Sci. USA **108**, 15097 (2011).

[10] S.-H. Su, C.-P. Sun, S.-W. Li, and J.-C. Chen, Phys. Rev. E **93**, 052103 (2016).

[11] D. Meschede, H. Walther, and G. Müller, Phys. Rev. Lett. **54**, 551 (1985).

[12] G. S. Agarwal, R. K. Bullough, and G. P. Hildred, Opt. Commun. **59**, 23 (1986).

[13] G. S. Agarwal and S. Dutta Gupta, Phys. Rev. A **42**, 1737 (1990).

[14] H. Walther, *Frontiers of Laser Physics and Quantum Optics* (Springer, Berlin, 2000), pp. 39–69.

[15] L. Teuber, P. Grünwald, and W. Vogel, Phys. Rev. A **92**, 053857 (2015).

[16] E. Boukobza and D. J. Tannor, Phys. Rev. A **74**, 063823 (2006).

[17] E. Boukobza and D. J. Tannor, Phys. Rev. A **74**, 063822 (2006).

[18] E. Boukobza and D. J. Tannor, Phys. Rev. Lett. **98**, 240601 (2007).

[19] S. Rahav, U. Harbola, and S. Mukamel, Phys. Rev. A **86**, 043843 (2012).

[20] Y. Perl, Y. B. Band, and E. Boukobza, Phys. Rev. A **95**, 053823 (2017).

[21] T. Yuge, M. Yamaguchi, and T. Ogawa, Phys. Rev. E **95**, 022119 (2017).

[22] M. H. Ansari, Phys. Rev. B **95**, 174302 (2017).

[23] M. Scully and W. E. Lamb, Phys. Rev. Lett. **16**, 853 (1966).

[24] M. O. Scully and W. E. Lamb, Phys. Rev. **159**, 208 (1967).

[25] M. O. Scully and M. S. Zubairy, *Quantum Optics* (Cambridge University Press, Cambridge, 1997).

[26] D. Yu and J. Chen, Phys. Rev. A **81**, 053809 (2010).

[27] M. Sargent, M. O. Scully, and W. E. Lamb, Jr., *Laser Physics*, 5th ed. (Westview, Boulder, 1978).